PCCP

PAPER

View Article Online
View Journal | View Issue

Cite this: *Phys. Chem. Chem. Phys.*, 2022, **24**, 19890

Iron L_3-edge energy shifts for the full range of possible 3d occupations within the same oxidation state of iron halides†

Max Flach, [ab] Konstantin Hirsch, [a] Martin Timm,[a] Olesya S. Ablyasova,[ab] Mayara da Silva Santos, [ab] Markus Kubin, [a] Christine Bülow,[ab] Tim Gitzinger,[ab] Bernd von Issendorff,[b] J. Tobias Lau *[ab] and Vicente Zamudio-Bayer [a]

Received 30th May 2022,
Accepted 31st July 2022

DOI: 10.1039/d2cp02448a

rsc.li/pccp

Oxidation states are integer in number but d^n configurations of transition metal centers vary continuously in polar bonds. We quantify the shifts of the iron L_3 excitation energy, within the same formal oxidation state, in a systematic L-edge X-ray absorption spectroscopy study of diatomic gas-phase iron(II) halide cations, $[FeX]^+$,where X = F, Cl, Br, I. These shifts correlate with the electronegativity of the halogen, and are attributed exclusively to a fractional increase in population of 3d-derived orbitals along the series as supported by charge transfer multiplet simulations and density functional theory calculations. We extract an excitation energy shift of 420 meV ± 60 meV spanning the full range of possible 3d occupations between the most ionic bond in $[FeF]^+$ and covalently bonded $[FeI]^+$.

Introduction

X-ray absorption spectroscopy at the $L_{2,3}$ edges of 3d transition metals is a widely adapted method to identify oxidation states in battery, catalysis, and materials research.[1–6] This is, because excitation energies as well as spectral signatures depend on 3d valence occupation numbers, which determine oxidation states. In addition, crystal structure, bond distance, crystal field, or spin state also contribute to a considerable spread of excitation energies within one formal oxidation state.[7–10]

Our aim is to isolate, and quantify, the variations in excitation energies as well as changes in spectral signature that are caused by modifying the 3d occupation only, without changing the formal oxidation state itself. Hence, we study diatomic iron halide cations $[Fe^{II}X]^+$ (X = F, Cl, Br, I)[11–13] where coordination number, charge state, symmetry and multiplicity remain unchanged, while the electronegativity (EN) of the halides decreases along the series. The variation of the EN systematically tunes the covalency of the bond and, therefore, the 3d occupation of the iron center. This enables us to effectively sample the full range of 3d occupations within the same formal oxidation state, since fluorine is the most electronegative element in the periodic table of elements, while iodine has an EN comparable to that of iron.

From a combined lifetime-broadening limited X-ray absorption spectroscopy, charge transfer multiplet (CTM), and density functional theory (DFT) study we find a spread in L-edge excitation energies within one oxidation state of 420 meV, caused by variations in the metal center 3d occupation only. This range is comparable in magnitude to the excitation energy variations observed in bulk samples[7,14] where the energy spread is subject to additional effects.

Experimental set up and methods

All experiments were performed at the ion-trap endstation of the UE52-PGM beamline at the BESSY II synchrotron radiation facility.[15] To produce molecular cations, two different techniques, electrospray ionization with an ion funnel interface[16,17] and magnetron sputtering in combination with a hexapole collision cell,[18] are used. The obtained spectra are identical for both ion sources as verified for the $[FeCl]^+$ ion.

Using the electrospray ionization source, the samples are produced from solutions of commercially available iron(II) halides in ultra pure water or methanol (see ESI,† Section 1.1) at typical concentrations of 1 mmol l^{-1} and at flow rates of 0.25 ml h^{-1}. For sample preparation by magnetron sputtering, iron cations are produced by argon sputtering of an iron target, and are exposed to the corresponding halomethane in a hexapole collision cell.

[a] *Abteilung für Hochempfindliche Röntgenspektroskopie, Helmholtz-Zentrum Berlin für Materialien und Energie, Albert-Einstein-Str. 15, 12489 Berlin, Germany. E-mail: tobias.lau@helmholtz-berlin.de*

[b] *Physikalisches Institut, Albert-Ludwigs-Universität Freiburg, Hermann-Herder-Str. 3, 79104 Freiburg, Germany*

† Electronic supplementary information (ESI) available: Details on sample preparation, error estimation, and charge transfer multiplet calculations. See DOI: https://doi.org/10.1039/d2cp02448a

In both cases, $[FeX]^+$ cations are mass selected by a quadrupole mass filter and are guided by radio frequency quadrupole and hexapole ion guides into a linear Paul trap for accumulation.[15] Cryogenic helium buffer gas cooling is used to thermalize the ions in the trap to a temperature of $\approx$ 10 K.[19] After X-ray absorption induced fragmentation of the parent molecular cations, the product ions are extracted into a time-of-flight mass spectrometer by a pulsed aperture. Mass spectra are recorded to detect the partial ion yield that is taken as a measure of the X-ray absorption cross section of the parent ion.[20]

The photon energy is scanned in steps of 30 meV, at a bandwidth of 80 meV, to measure the X-ray absorption spectra. This bandwidth is well below the iron 2p core hole lifetime broadening of approximately 400 meV[21,22] and therefore enables us to resolve the multiplet structure at the L_3 edge. In addition to the absolute photon energy calibration, for which the neon 1s excitation is used, a reference sample procedure is applied to reduce the error in relative energy of each spectra to below 45 meV (for details see ESI,† Sections 2.1 and 2.2). We can thus resolve relative shifts of L_3 excitation energy with high accuracy of 0.06 eV from our energy-calibrated data.

For comparison with the experimental data and to extract local 3d occupations, charge transfer multiplet calculations are performed with the CTM4XAS code,[23] taking electron–electron and spin–orbit coupling into account. The charge transfer parameter Δ and hopping terms T are used to simulate spectral changes along the series, see ESI,† Section 4.

To further support the results of the charge transfer multiplet calculations, 3d orbital occupation derived from DFT calculations and natural population analysis were obtained using turbomole version 7.5.1[24] employing the B3LYP functional[25] and the def2-TZVP basis set.[26]

Results and discussion

Experimental L_3 X-ray absorption spectra of $[FeX]^+$ (X = F, Cl, Br, I) in their $^5\Delta$ ground states[11–13] and, as reference, of the iron cation Fe^+ in its $3d^6\ 4s^1\ ^5D$ ground state are shown in Fig. 1. The latter was previously available in the literature only with lower resolution[21] or as a mixture of relaxed and metastable Fe^+ ions.[27] Lower resolution spectra of the whole Fe $L_{2,3}$ energy region can be found in the ESI.† While it appears possible to trace back the shape of the $[FeF]^+$ spectrum to the one of Fe^+, this does not apply anymore in the case of $[FeI]^+$.

The Fe L_3-edge intensity distribution in the X-ray absorption spectra of $[FeX]^+$ shifts towards lower excitation energies, as indicated by the median, from $[FeF]^+$ through $[FeI]^+$, see black lines in Fig. 1. Although the intensity maximum of the L_3 transitions is commonly used as a simple measure of excitation energy shifts,[7] here we use instead the median[5,28] as a robust measure of the final state energy distribution that can also be applied in cases where there is no distinct maximum, as for the L_3 spectrum of $[FeX]^+$. Significant shifts of the median are observed between all neighbors in the series except for $[FeCl]^+$ and $[FeBr]^+$, as can be seen in Fig. 1. Absolute energy calibration

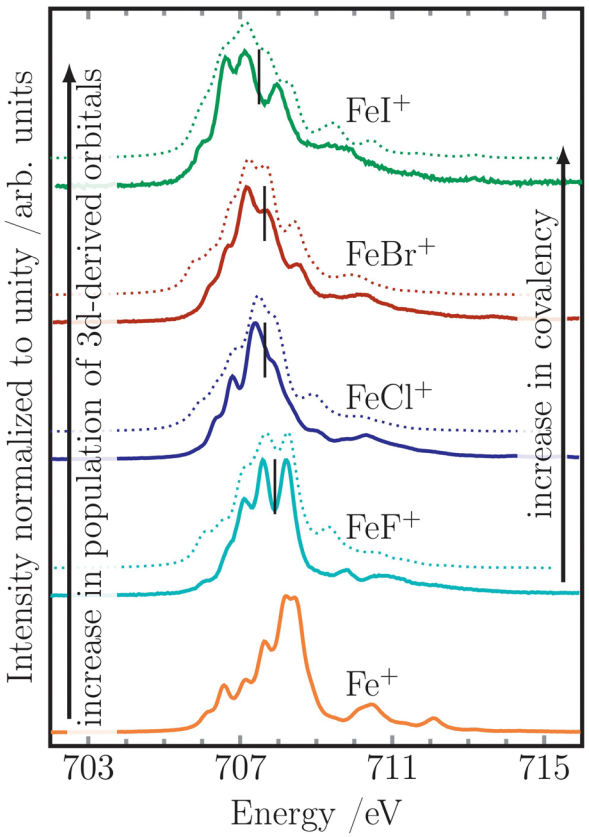

Fig. 1 Experimental iron L_3 excitation of Fe^+ and of $[FeX]^+$, X = F, Cl, Br, I (solid lines) and results from charge transfer multiplet calculations (dotted lines). Black vertical lines indicate the median of the experimental L_3 intensity distribution that shifts by 420 ± 60 meV towards lower energy from $[FeF]^+$ through $[FeI]^+$ as the covalency of the bond increases, and goes along with an increase in population of 3d derived orbitals, from 6.1 to 6.6 electrons, over the series. The results of our multiplet calculations are shifted to fit the energy positions of the experimental spectra. Spectra of the full $L_{2,3}$-edge are provided in the ESI,† Fig. S1.

and a thorough procedure to minimize uncertainty in relative energies, along with a high signal-to-noise ratio, enables us to extract quantitative shifts with an error in energy of less then 0.06 eV. Numerical values of the excitation energy shifts are given in Table 1. Across the $[FeX]^+$ series this shift has a magnitude of 420 ± 60 meV while the iron atom is in the same formal oxidation state of +2 in all iron halide samples.[29] These median L_3 excitation energies of $[FeX]^+$ are plotted against the

Table 1 Experimental values of the median L_3 excitation energy of the $[FeX]^+$ series. Energy differences to the L_3 median of $[FeF]^+$, and iron 3d derived orbital populations n from charge transfer multiplet calculations and DFT calculations for comparison

	L_3 median in eV	Shift relative to $[FeF]^+$ in eV	Iron 3d population n CTM	DFT
$[FeF]^+$	707.91 ± 0.04		6.1	6.34
$[FeCl]^+$	707.65 ± 0.04	−0.26 ± 0.05	6.3	6.53
$[FeBr]^+$	707.64 ± 0.04	−0.27 ± 0.06	6.3	6.57
$[FeI]^+$	707.49 ± 0.05	−0.42 ± 0.06	6.6	6.73

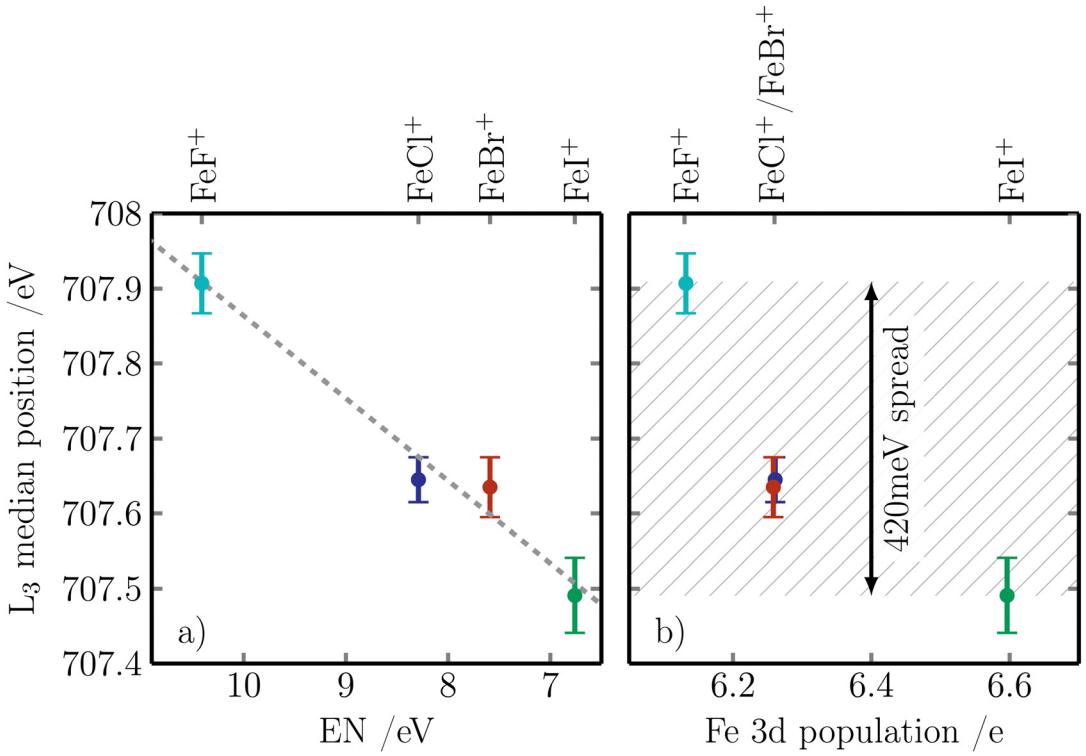

Fig. 2 (a) Median excitation energies of $[FeX]^+$ as function of halogen electronegativity in the Mulliken scale[30–33] as also given in Table 1. The dashed line is a guide to the eye. The electronegativity scale is inverted to stress the connection with local 3d occupation as shown in panel b. (b) Median L_3 excitation energies of $[FeX]^+$ as function of the local 3d population at the iron center, as extracted from charge transfer multiplet simulations. A shift in excitation energy of 420 meV ± 60 meV between $[FeF]^+$, with the most ionic bond, and $[FeI]^+$, with an almost purely covalent bond, can be seen. The characterization of the bond as ionic and covalent is substantiated by the 3d occupations as extracted from charge transfer multiplet simulations.

Mulliken EN[30] of the halogen[31–33] in Fig. 2(a). As expected, the excitation energy shifts towards lower energies with decreasing EN of the halogen.

Furthermore, the photon energy bandwidth used to record the X-ray absorption spectra, well below the natural width of a single multiplet transition,[21,22] allows us to simulate with good agreement the resolved multiplet spectral signature, using a parametrized CTM model[23] as shown in Fig. 1. Since the absolute excitation energies obtained from parametrized CTM calculations are known to be unreliable[34] the simulated spectra have been shifted to fit the experimental data (see ESI† for further details). Nevertheless, the CTM simulations permit us, because of characteristic spectral shapes, to deduce 3d occupations of the iron center along the $[FeX]^+$ series. It is worth pointing out here that the experimental core excited spectra can be well reproduced even without invoking any crystal field splitting, indicating that these effects can be neglected for $[FeX]^+$ series, which is also expected since halogens are weak ligands in the spectrochemical series. This, in turn, provides further evidence that only the 3d occupation of the metal center is changed. The values for the iron 3d occupation along the series show qualitatively the same monotonous trend as a function of EN as 3d occupations extracted from population analysis of DFT calculations of $[FeX]^+$, shown in Table 1. Therefore the L_3 excitation energy can also be plotted against the 3d occupation as shown in Fig. 2(b) in an approach that has been foreshadowed in ref. 14 and 35. Moreover, the determined 3d occupations indicate that we probe the whole range of possible 3d occupations within a single formal oxidation state: From the most ionic bond in $[FeF]^+$, with fluorine being the most electronegative element of the periodic table, to a covalent bond in $[FeI]^+$ as substantiated by the extracted 3d occupation number indicating equal sharing of an electron. The variation in 3d occupation across the $[FeX]^+$ series results in an energy spread of the excitation energy at the iron $L_{2,3}$ edges of 420 meV ± 60 meV.

Conclusion

We have quantified the energy variation of excitation energies at the L_3 edge of diatomic iron halide cations that is solely determined by the change in 3d occupation within the same formal oxidation state. Interestingly, the extracted energy spread across the whole span of possible 3d occupations of 420 meV ± 60 meV has the same order of magnitude as energy spreads determined in bulk samples within the same oxidation state.[7,36] In the latter cases, the variation cannot be traced back to a single origin, as many other effects can obscure the shifts induced by changes in 3d occupation alone.[7,36] Furthermore, the variation of excitation energies within one formal oxidation state is also sizable compared to the shifts between different formal oxidation states that are of the order of 1—2 eV per oxidation state,[5,28,36–39] again highlighting that the excitation

energy shift must be complemented by additional data in order to reliably extract information on the oxidation state.[7,8]

With the rich multiplet structure resolved, which is very sensitive to the iron 3d occupation, the energy-calibrated high-resolution spectra of ground state Fe^+ and $[FeX]^+$ ions can serve as benchmarks for high level quantum theory approaches to further improve on simultaneously reproducing both, spectral signatures and total excitation energies of open shell systems.[40]

Author contributions

JTL, MF, and VZB devised the project, designed the experimental study, and prepared the beamtime proposal along with BvI, MK, and MT. BvI, JTL, KH, MF, MT, and VZB designed the experimental setup. BvI and JTL acquired funding for its realization. CB, MF, MK, MSS, MT, OSA, TG, and VZB prepared all samples, performed the experiments, and validated their reproducibility. MF analyzed and visualized the data under guidance of JTL, KH, and VZB. KH and MF performed the calculations. JTL, KH, MF, and VZB validated the methods and results. JTL, KH, and VZB supervised the project. MF wrote the original draft, with reviewing and editing by JTL, KH, and VZB.

Conflicts of interest

There are no conflicts to declare.

Acknowledgements

This project has received funding from the German Federal Ministry of Education and Research (BMBF) through Grant no. BMBF-05K16Vf1. Beamtime for this project was granted by HZB at beamline UE52-PGM ion trap of the BESSY II synchrotron radiation facility. BvI, JTL, MF, and OSA acknowledge support by Deutsche Forschungsgemeinschaft (DFG) within RTG 2717.

References

1 F. Yang, X. Feng, Y.-S. Liu, L. C. Kao, P.-A. Glans, W. Yang and J. Guo, *Energy Environ. Mater.*, 2021, **4**, 139–157.
2 M. F. Tesch, S. A. Bonke, T. E. Jones, M. N. Shaker, J. Xiao, K. Skorupska, R. Mom, J. Melder, P. Kurz, A. Knop-Gericke, R. Schlögl, R. K. Hocking and A. N. Simonov, *Angew. Chem., Int. Ed.*, 2019, **58**, 3426–3432.
3 X. Zheng, B. Zhang, P. De Luna, Y. Liang, R. Comin, O. Voznyy, L. Han, F. P. García de Arquer, M. Liu, C. T. Dinh, T. Regier, J. J. Dynes, S. He, H. L. Xin, H. Peng, D. Prendergast, X. Du and E. H. Sargent, *Nat. Chem.*, 2018, **10**, 149–154.
4 W. Yang and T. P. Devereaux, *J. Power Sources*, 2018, **389**, 188–197.
5 M. Risch, K. A. Stoerzinger, B. Han, T. Z. Regier, D. Peak, S. Y. Sayed, C. Wei, Z. Xu and Y. Shao-Horn, *J. Phys. Chem. C*, 2017, **121**, 17682–17692.
6 X. Liu, D. Wang, G. Liu, V. Srinivasan, Z. Liu, Z. Hussain and W. Yang, *Nat. Commun.*, 2013, **4**, 2568.
7 T. L. Daulton and B. J. Little, *Ultramicroscopy*, 2006, **106**, 561–573.
8 R. G. Castillo, A. W. Hahn, B. E. Van Kuiken, J. T. Henthorn, J. McGale and S. DeBeer, *Angew. Chem., Int. Ed.*, 2021, **60**, 10112–10121.
9 A. E. Bocquet, T. Mizokawa, T. Saitoh, H. Namatame and A. Fujimori, *Phys. Rev. B: Condens. Matter Mater. Phys.*, 1992, **46**, 3771–3784.
10 G. van der Laan and B. T. Thole, *Phys. Rev. B: Condens. Matter Mater. Phys.*, 1991, **43**, 13401.
11 C. W. Bauschlicher, *Chem. Phys.*, 1996, **211**, 163–169.
12 W. S. Taylor, R. E. Pedder, A. B. Eden and C. L. Emmerling, *J. Phys. Chem. A*, 2018, **122**, 6509–6523.
13 R. D. Bach, D. S. Shobe, H. B. Schlegel and C. J. Nagel, *J. Phys. Chem.*, 1996, **100**, 8770–8776.
14 W. Gu, H. Wang and K. Wang, *Dalton Trans.*, 2014, **43**, 6406–6413.
15 K. Hirsch, J. T. Lau, P. Klar, A. Langenberg, J. Probst, J. Rittmann, M. Vogel, V. Zamudio-Bayer, T. Möller and B. von Issendorff, *J. Phys. B: At., Mol. Opt. Phys.*, 2009, **42**, 154029.
16 D. Egorov, B. Sadia, R. Hoekstra, A. Lawicki, K. Hirsch, V. Zamudio-Bayer, T. Lau, B. von Issendorf and T. Schlathölter, *J. Phys.: Conf. Ser.*, 2015, **635**, 112083.
17 S. Bari, D. Egorov, T. L. C. Jansen, R. Boll, R. Hoekstra, S. Techert, V. Zamudio-Bayer, C. Bülow, R. Lindblad, G. Leistner, A. awicki, K. Hirsch, P. S. Miedema, B. von Issendorff, J. T. Lau and T. Schlathölter, *Chem. – Eur. J.*, 2018, **24**, 7631.
18 S. T. Akin, V. Zamudio-Bayer, K. Duanmu, G. Leistner, K. Hirsch, C. Bülow, A. awicki, A. Terasaki, B. von Issendorff, D. G. Truhlar, J. T. Lau and M. A. Duncan, *J. Phys. Chem. Lett.*, 2016, **7**, 4568–4575.
19 V. Zamudio-Bayer, R. Lindblad, C. Bülow, G. Leistner, A. Terasaki, B. V. Issendorff and J. T. Lau, *J. Chem. Phys.*, 2016, **145**, 194302.
20 J. T. Lau, J. Rittmann, V. Zamudio-Bayer, M. Vogel, K. Hirsch, P. Klar, F. Lofink, T. Möller and B. V. Issendorff, *Phys. Rev. Lett.*, 2008, **101**, 153401.
21 K. Hirsch, V. Zamudio-Bayer, F. Ameseder, A. Langenberg, J. Rittmann, M. Vogel, T. Möller, B. V. Issendorff and J. T. Lau, *Phys. Rev. A: At., Mol., Opt. Phys.*, 2012, **85**, 062501.
22 P. Gambardella, S. S. Dhesi, S. Gardonio, C. Grazioli, P. Ohresser and C. Carbone, *Phys. Rev. Lett.*, 2002, **88**, 047202.
23 E. Stavitski and F. M. de Groot, *Micron*, 2010, **41**, 687–694.
24 M. Von Arnim and R. Ahlrichs, *J. Comput. Chem.*, 1998, **19**, 1746–1757.
25 P. J. Stephens, F. J. Devlin, C. F. Chabalowski and M. J. Frisch, *J. Phys. Chem.*, 1994, **98**, 11623–11627.
26 F. Weigend and R. Ahlrichs, *Phys. Chem. Chem. Phys.*, 2005, **7**, 3297–3305.
27 S. Schippers, M. Martins, R. Beerwerth, S. Bari, K. Holste, K. Schubert, J. Viefhaus, D. W. Savin, S. Fritzsche and A. Müller, *Astrophys. J.*, 2017, **849**, 5.
28 F. Bourdelle, E. Lloret, C. Durand and L. Airaghi, *Phys. Chem. Miner.*, 2021, **48**, 18.

29 P. Karen, P. McArdle and J. Takats, *Pure Appl. Chem.*, 2014, **86**, 1017–1081.
30 R. S. Mulliken, *J. Chem. Phys.*, 1934, **2**, 782–793.
31 R. S. Berry and C. W. Reimann, *J. Chem. Phys.*, 1963, **38**, 1540–1543.
32 A. Kramida, Yu Ralchenko, J. Reader and NIST ASD Team, *NIST Atomic Spectra Database (ver. 5.8)*, [Online]. Available: **https://physics.nist.gov/asd** [2021, August 17]. National Institute of Standards and Technology, Gaithersburg, MD, 2020.
33 X. Chen, Z. Luo, J. Li and C. Ning, *Sci. Rep.*, 2016, **6**, 24996.
34 F. M. F. de Groot, J. C. Fuggle, B. T. Thole and G. A. Sawatzky, *Phys. Rev. B: Condens. Matter Mater. Phys.*, 1990, **42**, 5459–5468.
35 K. Yamagami, S. Imada, K. Yamanaka, T. Yaji, A. Tanaka, M. Kouno, N. Yoshinari, T. Konno and A. Sekiyama, *J. Phys. Commun.*, 2019, **3**, 125008.
36 H. Tan, J. Verbeeck, A. Abakumov and G. Van Tendeloo, *Ultramicroscopy*, 2012, **116**, 24–33.
37 S. P. Cramer, F. M. F. DeGroot, Y. Ma, C. T. Chen, F. Sette, C. A. Kipke, D. M. Eichhorn, M. K. Chan, W. H. Armstrong, E. Libby, G. Christou, S. Brooker, V. McKee, O. C. Mullins and J. C. Fuggle, *J. Am. Chem. Soc.*, 1991, **113**, 7937–7940.
38 J. K. Kowalska, B. Nayyar, J. A. Rees, C. E. Schiewer, S. C. Lee, J. A. Kovacs, F. Meyer, T. Weyhermüller, E. Otero and S. DeBeer, *Inorg. Chem.*, 2017, **56**, 8147–8158.
39 M. Kubin, M. Guo, M. Ekimova, M. L. Baker, T. Kroll, E. Källman, J. Kern, V. K. Yachandra, J. Yano, E. T. J. Nibbering, M. Lundberg and P. Wernet, *Inorg. Chem.*, 2018, **57**, 5449–5462.
40 M. Guo, E. Källman, R. V. Pinjari, R. C. Couto, L. Kragh Sørensen, R. Lindh, K. Pierloot and M. Lundberg, *J. Chem. Theory Comput.*, 2019, **15**, 477–489.